

Membrane-inlet mass spectrometry reveals a high driving force for oxygen production by photosystem II

Dmitriy Shevela^{a,b,1}, Katrin Beckmann^b, Jürgen Clausen^c, Wolfgang Junge^{c,2}, and Johannes Messinger^{a,b,2}

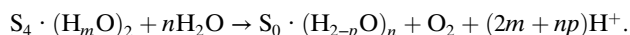
^aInstitutionen för Kemi, Kemiskt Biologiskt Centrum (KBC), Umeå Universitet, Linnaeus väg 6, S-90187 Umeå, Sweden; ^bMax-Planck-Institut für Bioanorganische Chemie, Stiftstrasse 34-36, D-45470 Mulheim an der Ruhr, Germany; and ^cAbteilung Biophysik, Fachbereich Biologie/Chemie, Universität Osnabrück, D-49069 Osnabrück, Germany

Edited* by Pierre A. Joliot, Institut de Biologie Physico-Chimique, Paris, France, and approved January 10, 2011 (received for review September 23, 2010)

Oxygenic photosynthesis is the basis for aerobic life on earth. The catalytic Mn_4O_xCa center of photosystem II (PSII), after fourfold oxidation, extracts four electrons from two water molecules to yield dioxygen. This reaction cascade has appeared as a single four-electron transfer that occurs in typically 1 ms. Inevitable redox intermediates have so far escaped detection, probably because of very short lifetime. Previous attempts to stabilize intermediates by high O_2 -back pressure have revealed controversial results. Here we monitored by membrane-inlet mass spectrometry (MIMS) the production of $^{18}O_2$ from ^{18}O -labeled water against a high background of $^{16}O_2$ in a suspension of PSII-core complexes. We found neither an inhibition nor an altered pattern of O_2 production by up to 50-fold increased concentration of dissolved O_2 . Lack of inhibition is in line with results from previous X-ray absorption and visible-fluorescence experiments, but contradictory to the interpretation of previous UV-absorption data. Because we used essentially identical experimental conditions in MIMS as had been used in the UV work, the contradiction was serious, and we found it was not to be resolved by assuming a significant slowdown of the O_2 release kinetics or a subsequent slow conformational relaxation. This calls for reevaluation of the less direct UV experiments. The direct detection of O_2 release by MIMS shows unequivocally that O_2 release in PSII is highly exothermic. Under the likely assumption that one H^+ is released in the $S_4 \rightarrow S_0$ transition, the driving force at pH 6.5 and atmospheric O_2 pressure is at least 220 meV, otherwise 160 meV.

water oxidation | oxygen evolution | isotope-ratio mass spectrometry | bioenergetics

Oxygenic photosynthesis is the metabolic basis for the most successful forms of life on earth. In cyanobacteria, algae and plants photosystem II (PSII) uses sunlight to split water into dioxygen and reducing equivalents, and it generates proton motive force. The catalytic centre of O_2 production in PSII, coined the OEC (oxygen evolving complex), comprises the manganese–oxygen–calcium (Mn_4O_xCa) complex and its ligands, which include two substrate “water” molecules of undefined protonation state. It also includes a redox-active tyrosine residue, coined tyrosine Z (Y_Z), which is the essential electron transfer link to the photoactive reaction center of PSII. Over 40 years ago Kok et al. (1) proposed—on the basis of flash-induced O_2 -evolution patterns (2)—that PSII, clocked and driven by four quanta of light, cycles through five different redox states, named S_i ($i = 0, \dots, 4$), where i is the number of stored oxidizing equivalents. Once four oxidizing equivalents are accumulated O_2 is produced in the spontaneous reaction from S_4 to yield S_0 .



[1]

In this S_i state transition four electrons are transferred from two bound substrate water molecules that were partially or fully deprotonated ($m = 0-2$) during the S_i state cycle. In addition, one or two new substrate water molecules ($n = 1, 2$) bind to

the Mn_4O_xCa cluster under the release of np protons into the medium ($p = 0-2$) (3–5). In general the release of two protons is observed for the $S_3 \rightarrow S_4 \rightarrow S_0$ transition (6), of which one is expelled after $S_3Y_Z^{ox}$ formation (7, 8), the highest oxidation state characterized so far by spectroscopy. It appears that reaction 1 occurs significantly faster than the formation of S_4 from $S_3Y_Z^{ox}$ (see ref. 3 for a recent review).

For decades it has appeared as if the four electrons were transferred in reaction 1 in one batch, because three different events proceeded with the same half-rise time, typically 1–1.5 ms, namely (i) the appearance of O_2 in solution, (ii) the reduction of Y_Z^{ox} , and (iii) the reduction of the Mn_4O_xCa cluster in the S_3 state. This coincidence has been well documented by a wealth of independent techniques. (i) The appearance of O_2 in solution was time resolved by four different techniques, namely continuous flow (9), EPR (10, 11), polarography with a bare Pt electrode (2, 12–14) and via absorption changes of intracellular cytochrome *c* oxidase (15). (ii) The reduction of Y_Z^{ox} was detected by time-resolved EPR (10, 16, 17), and (iii) the reduction of the Mn_4O_xCa cluster by UV absorption (7, 12, 18–20), delayed chlorophyll fluorescence (DF) (21), and time-resolved Mn-K-edge spectroscopy (8, 22). Based on general considerations, however, a direct four-electron transfer from water to the $Mn_4O_xCaY_Z^{ox}$ moiety is improbable, redox intermediates inevitably exist, and it is pivotal for understanding the mechanism of water oxidation to characterize their chemical nature.

In an attempt to stabilize putative redox intermediates (S_4^n states) of the reaction $Y_Z^{ox}S_3 \rightarrow Y_ZS_4 \rightarrow Y_ZS_0$ two of us (23) applied elevated O_2 back pressure and found that the characteristic millisecond component of UV-absorption transients [that has been attributed to Mn oxidoreduction (18)] was half suppressed if the O_2 pressure was raised only 10-fold above the atmospheric level (2.3 bars versus 0.21 bar). DF studies corroborated these effects of moderately elevated O_2 pressure on the OEC (21). Experiments by time-resolved K-edge X-ray absorption spectroscopy (TR-XAS), which directly monitored the Mn-oxidoreduction, indicated a changed dark-equilibrium between S_i states or changes in the flash-induced turnover efficiencies of PSII, but neither a blockade nor a significant slowing of the $S_3 \rightarrow S_0$ transition in response to elevated O_2 levels (22). All the above cited studies were carried out with isolated PSII-core complexes (PSII-cc) of *Synechocystis* sp. PCC 6803 (*Syn. sp.*) or spinach PSII membrane fragments (PSII-mf).

Author contributions: D.S., K.B., J.C., W.J., and J.M. designed research; D.S., K.B., and J.C. performed research; D.S., W.J., and J.M. analyzed data; and D.S., W.J., and J.M. wrote the paper.

The authors declare no conflict of interest.

*This Direct Submission article had a prearranged editor.

¹Present address: Center for Organellar Research, University of Stavanger, Kristine Bonnevis vei 22, N-4036 Stavanger, Norway.

²To whom correspondence may be addressed. E-mail: junge@uos.de or johannes.messinger@chem.umu.se.

This article contains supporting information online at www.pnas.org/lookup/suppl/doi:10.1073/pnas.1014249108/-DCSupplemental.

If the inhibition by elevated O_2 pressure holds true for whole cells or intact leaves, photosynthesis could not raise the atmospheric O_2 content of the atmosphere much above its present level (23). The prospect of such a rather strict boundary condition for past and future evolution of life on earth has provoked vivid discussion (24–28), and a recent study on the operation of the OEC in various plants, algae, and cyanobacteria has shed doubt on such limitation (29). The matter has remained controversial because in all the above cited studies on the effects of elevated O_2 pressure, the release of O_2 was not detected directly, and different sample materials (species and type of preparation) were used. This has prompted us to monitor O_2 production from $H_2^{18}O$ by membrane-inlet mass spectrometry (MIMS) as a function of the $^{na}O_2$ pressure (na, natural abundance, hereafter simply denoted as O_2). Scrutinizing the specific results and conclusions of previous studies (21–23, 30), the experiments were carried out under basically identical experimental boundary conditions (pH, temperature, and buffer composition), and by using samples from the same stock of frozen *Syn. sp.* PSII-cc as employed in ref. 23.

Results

Enrichment of PSII Suspension with O_2 . The equilibration of PSII suspensions in a buffer containing 100 mM sucrose, 25 mM $CaCl_2$, 10 mM NaCl, 1 M glycine betaine, 50 mM MES (pH 6.7 or 5.5) and 30–50% $H_2^{18}O$ with O_2 or N_2 at the applied pressure in the gas phase of a specially developed reaction cell (Fig. 1) was monitored by MIMS. Fig. 2 shows the time course of the enrichment of the PSII suspension with O_2 at 20 bars pressure. After about 35 min exposure to 20 bars, the $^{16}O_2$ concentration increased 50–60 times over the ambient initial $^{16}O_2$ level (~ 0.21 bar). Assuming a linear response to the dissolved $^{16}O_2$ of the MIMS output signal and the validity of Henry's law the saturation level corresponds to at least 10 bars, i.e., to about 50% of the expected level. This is a lower estimate because calibration measurements (see *Materials and Methods* and Fig. S1) show that the sensitivity of our MIMS setup is reduced by 20–40% at 20 bars. Although it is difficult to determine the exact concentration of dissolved O_2 at high pressure, it is important to emphasize that even this lowest estimate (equivalent to 10 bars) is high enough to probe the previously reported effects, which suggest that half-inhibition of O_2 evolution by PSII occurs at 2.3 bars O_2 . In the following, we therefore simply report the

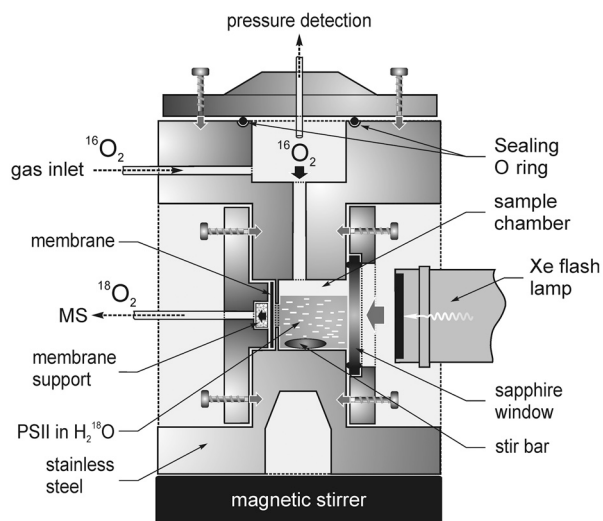


Fig. 1. Pressure cell for the MIMS measurements of flash-induced O_2 -evolving activity of PSII samples at O_2/N_2 pressures up to 20 bars. For details, see *Materials and Methods*.

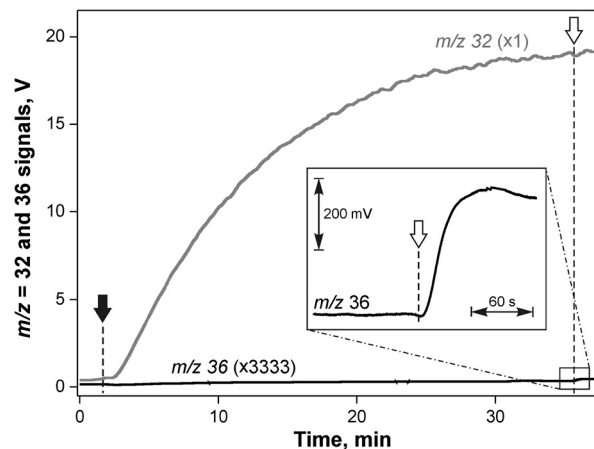


Fig. 2. Rise of dissolved $^{16}O_2$ ($m/z = 32$) in the suspension of PSII-cc from *Syn. sp.* upon application of 20 bars O_2 pressure (closed arrow) monitored by MIMS. (Inset) The zoomed region of $^{18}O_2$ evolution ($m/z = 36$) induced by 30 Xe flashes (2 Hz; open arrow). Values in brackets indicate MS Faraday cup amplification. Other conditions: $\sim 50\%$ $H_2^{18}O$, $[Chl] = 5 \mu M$ Chl, 250 μM DCBQ, pH 6.7, 20 $^\circ C$.

admitted pressure in the gas phase, and not the achieved partial pressure in solution.

Fig. 2 also shows that although the signal for $^{16}O_2$ slowly increased, the level of the $m/z = 36$ signal remained almost stable at a very low level. The initial amplitude of the 36 signal is dominated by the ^{36}Ar isotope (0.337% na) in air. The concentration of Ar declines with time by degassing into the mass spectrometer, but this is almost compensated by the increasing level of $^{18}O_2$, which occurs with low natural abundance ($\sim 0.0004\%$). The rise of the O_2 concentration at $m/z = 34$ was always simultaneously recorded and gave consistent data (Fig. S2, Inset). To separate pressure-induced effects on the MIMS apparatus or on the OEC from O_2 -specific effects, control experiments were performed under $^{na}N_2$ pressure (hereafter N_2). The enrichment of the PSII suspension with $^{14}N_2$ was also monitored by MIMS (Fig. S2).

Photosynthetic O_2 Evolution at Atmospheric and Elevated O_2/N_2 Pressures. The experiments reported below were performed after the saturation of the gas solubility was reached (monitored as in Fig. 2), i.e., after 35–50 min of stirring in the dark. O_2 -evolution activity of PSII was then probed by illumination with Xe flashes: At $m/z = 32$ the MIMS signal was indistinguishable from noise, at $m/z = 34$ excitation with 30 flashes produced a discernible signal (see Fig. S2, Inset), and at $m/z = 36$ a large signal well above the low background was observed due to the high enrichment of the suspension with $H_2^{18}O$ (see Fig. 2, Inset).

Fig. 3 shows the $^{18}O_2$ -evolving activity of dark-adapted PSII-core particles in response to a series of 200 Xe flashes (2 Hz) for three different conditions in the gas phase, namely under air (1 bar, 0.21 bar O_2), O_2 (21.7 bars), and N_2 (20 bars). Under all three conditions light-induced $^{18}O_2$ evolution was observed, but the extent of the $m/z = 36$ signals at high pressure was by 20–25% smaller than at atmospheric pressure. Because this holds true for both O_2 and N_2 , this was attributed to an effect of pressure on the sensitivity of the MIMS apparatus rather than to a chemical effect of O_2 on the OEC. This assignment is in full agreement with the observed lower sensitivity of our MIMS setup toward $^{16}O_2$ at high applied pressures (see *Materials and Methods* and Fig. S1). The relative magnitudes of the $^{18}O_2$ release as documented in Fig. 3, i.e., 100% (air), 79% (O_2 , 20 bars), and 75% (N_2 , 20 bars), were reproducible with a standard deviation of 5% ($n = 4$). As a control in all cases $m/z = 40$ (Ar) traces were recorded, and one example is shown in Fig. 3. This documents

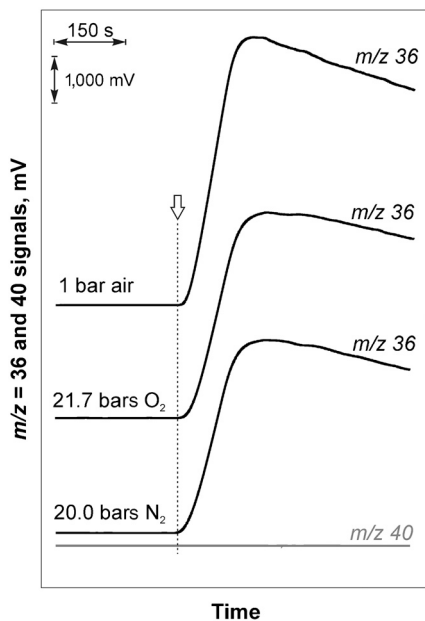


Fig. 3. $^{18}\text{O}_2$ evolution of PSII-cc from *Syn. sp.* induced by a series of 200 saturating Xe flashes (2 Hz; open arrow) at 1 bar air, 21.7 bars O_2 , or 20 bars N_2 . The time dependence of the Ar level ($m/z = 40$) is presented by a gray line. Other conditions: see Fig. 2, but $\sim 30\%$ H_2^{18}O and $[\text{Chl}] = 50 \mu\text{M}$.

the absence of changes in the gas permeability of the MIMS inlet during the measurements.

It is therefore obvious that, in contrast to expectations based on the previous UV measurements, there is no major specific effect of O_2 pressure (up to 20 bars) versus N_2 pressure on the extent of photosynthetic O_2 evolution under repetitive excitation at 2-Hz frequency.

The Influence of Flash Frequency and pH. One difference between the above experiments (Figs. 2 and 3) and the original UV-absorption data (23) is the frequency of flash excitation (2 Hz in this work versus 10 Hz in the former). This raised the possibility that an O_2 -induced kinetic limitation may have caused the previously observed inhibition. In order to address this question, experiments were performed using 20 flashes at 50-Hz frequency that were followed by 30 flashes at 2 Hz. The normalization of the former to the latter MIMS signals eliminated the unspecific pressure effects (see above). The normalized signal levels of 50-Hz traces obtained at 20 bars O_2 and 17 bars N_2 (Fig. 4A) were 40.2 (0.5) and 40.8 (1.0), respectively, where the numbers in parentheses give the standard deviation ($n = 2$). It was noteworthy that also under these conditions no O_2 -specific inhibition was observed, which exceeded the kinetic limitations of the acceptor

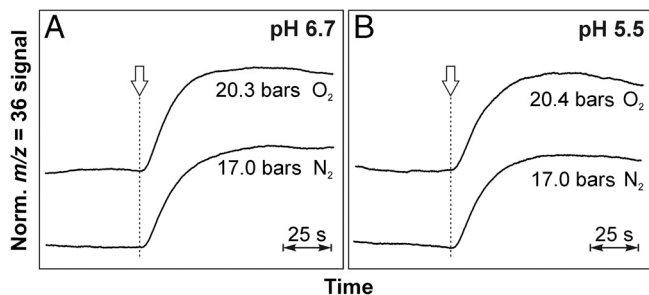


Fig. 4. Flash-induced $^{18}\text{O}_2$ evolution of PSII-cc from *Syn. sp.* measured by MIMS at 20 bars O_2 , or 17 bars N_2 and pH 6.7 (A) or pH 5.5 (B). $^{18}\text{O}_2$ evolution was induced by a series of 20 Xe flashes (arrows) given at 50 Hz. Other conditions: see Fig. 2. All data normalized to a consecutive series of 30 flashes at 2 Hz.

side electron transfer to 2,5-dichloro-*p*-benzoquinone (DCBQ) that caused the above signal levels to be below the theoretical value of about 67% (20/30).

In previous UV experiments it was observed that lowering the pH from 6.7 to 5.5 mimics the effect of elevated O_2 pressure on the OEC (30). This is plausible because a pH jump by one unit can exert a similar back pressure on the $\text{S}_4 \rightarrow \text{S}_0$ transition as a tenfold increased O_2 pressure, assuming one proton is released during the $\text{S}_4 \rightarrow \text{S}_0$ step (reaction 1). In order to maximize the back pressure, we explored by MIMS the combined effect of O_2 pressure and reduced pH. Again, no O_2 -specific inhibition was observed at 50 Hz (Fig. 4B) and at 2 Hz (Fig. S3) that exceeded the reduction of $\sim 35\%$ caused by the lower pH alone.

Flash-Induced Oxygen-Evolution Patterns (FIOPs). If PSII is dark-adapted under ambient air pressure, the OEC is predominantly in the S_1 state, such that the release of O_2 occurs after absorption of the third flash in a row, but negligibly after the second. Based on time-resolved X-ray absorption measurements, Haumann et al. proposed that exposure to elevated O_2 pressure (11–13 bars) causes either a shift of the S_i state distribution in the dark (30–40% from S_1 toward S_2) or an increase of photophysical double hits from normally 0–3% to about 15% (22). The double hit factor gives the percentage of centers that have been excited twice in a single flash (for details see ref. 3). Both effects imply that a considerable amount of O_2 would be produced already by the second flash of light.

Because a drastic change in the dark S_i state distribution or of the miss or double hit parameters could in principle also explain the previous UV observations, we scrutinized this possibility by MIMS. We first tried obtaining a flash pattern of PSII-cc. This is complicated, because due to the slow diffusion of O_2 through the MIMS membrane, dark times between the flashes of 25 s have to be employed in order to resolve the individual flash yields. Although the obtained flash pattern under 1 bar air, 20 bars O_2 , and 17 bars N_2 all looked identical, they were highly damped, most likely due to fast back reactions during the long dark periods (see Fig. S4). We therefore repeated these experiments with PSII-mf. Fig. 5A shows that the normalized FIOPs at 20 bars N_2 and 20 bars O_2 are practically identical. We further tested if the absence of an increased second flash O_2 yield holds true also for PSII-cc by measuring the sum of the O_2 yields obtained after excitation of dark-adapted samples with either two or three flashes of light given at 10 Hz (Fig. 5B). There was negligible $^{18}\text{O}_2$ production in the former and considerable in the latter case. This holds true both for equilibration with 1 bar air (0.21 bar O_2) and with 20 bars O_2 . In other words there was no evidence, by MIMS experiments, for the postulated S_i state shift (22) by elevated $^{16}\text{O}_2$ pressure of the flash pattern of $^{18}\text{O}_2$ release. In addition, no evidence for effects of elevated O_2 pressure on the miss and double hit parameters was found.

Discussion

In the MIMS experiments of this work the transient O_2 evolution and the concentration of dissolved O_2 in the PSII suspensions were directly detected and studied as a function of the O_2 pressure in the adjacent gas phase. We found both the extent of the $^{18}\text{O}_2$ -MIMS signals and its distribution over sequential flashes unimpaired by an at least 50-times increased O_2 concentration in the suspension. Below we discuss these findings in relation to the conflicting results of previous studies on this topic. Such conflicts may have three reasons: (i) mismatch between experimental boundary conditions, (ii) misconception in the interpretation of either data, or (iii) necessity to revise the present understanding of the addressed mechanism.

(i) Equivalence of the Experimental Boundary Conditions? The chemical boundary conditions in MIMS experiments were essentially

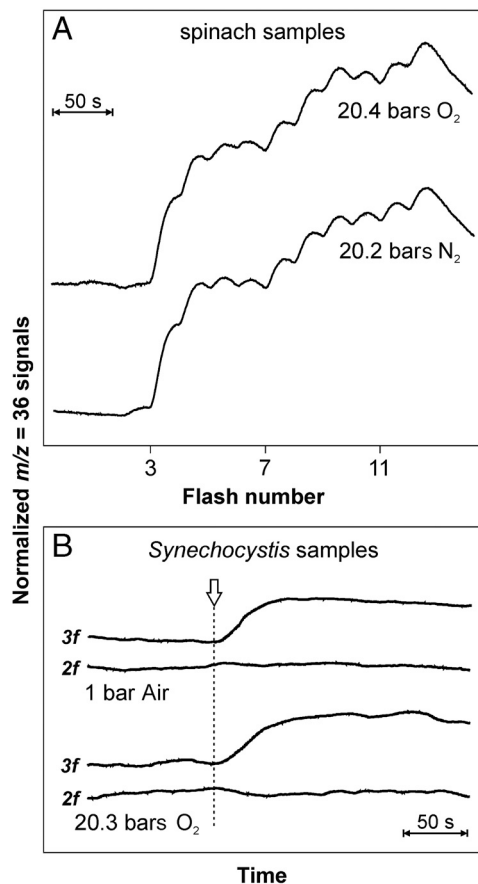


Fig. 5. $^{18}\text{O}_2$ evolution measured by MIMS at elevated (and normal) O_2 -(N_2 -) back pressure at $m/z = 36$ (A) FIOPs measured with PSII-mf from spinach at 20.4 bars O_2 or 20.2 bars N_2 . $^{18}\text{O}_2$ evolution was induced by a series of saturating laser flashes separated by dark times of 25 s. Other conditions: $\sim 40\%$ H_2^{18}O ; $[\text{Chl}] = 50 \mu\text{M}$; $1 \text{ mM } K_3[\text{Fe}(\text{CN})_6]$; pH 6.5; 20°C . (B) $^{18}\text{O}_2$ evolution induced by two (2f) or three (3f) Xe flashes (10 Hz) measured by MIMS in PSII-cc from *Syn. sp.* at 0.2 bar or at 20.3 bars O_2 . Other conditions: see Fig. 2, but $\sim 40\%$ H_2^{18}O and $[\text{Chl}] = 50 \mu\text{M}$. Data in both panels normalized as in Fig. 4.

the same as in the previous UV-spectroscopic work (23) (for a detailed comparison, see *SI Text* and *Figs. S5–S7*). Still we found (by MIMS) that O_2 production by PSII was not suppressed by elevated O_2 pressure as postulated in refs. 21 and 23, not even at acidic pH as in ref. 30. The MIMS results are thus in sharp contrast to the conclusions based on previous UV and DF studies (21, 23, 30), being in line with recent fluorescence (29) and TR-XAS experiments (22). The latter experiments showed at slightly different conditions (sample type, concentration, buffers, and acceptors; see *Table S1*) that the S_i state transitions are not blocked and that the Mn reduction during the S_4 - S_0 transition occurs with unchanged rate and amplitude. Our present MIMS data show in addition that neither the formation nor the unbinding of O_2 from the $\text{Mn}_4\text{O}_x\text{Ca}$ cluster are impaired by up to 50-fold elevated O_2 pressure.

However, there are also some minor discrepancies among the latter results. Whereas Haumann et al. (22), in their TR-XAS experiments, gave evidence for either an increased S_2 state dark population or an increased double hit parameter under 11–13 bars O_2 pressure, Kolling et al. (29), who monitored the pattern of variable fluorescence as a function of the flash number, found no changes in the oscillation patterns in thylakoids, under O_2 pressures up to 20 bars. Whereas the latter was coincident with our results, the former was not. Our finding of an unperturbed pattern of O_2 production (maxima upon

flashes 3, 7, 11,...) together with the data by Kolling et al. (29) dismiss the notion that the UV-absorption study might have been compromised by an influence of elevated O_2 pressure on the double hit factor or the miss parameter or other changes to the oscillation pattern. They rather support the possibility already considered by Haumann et al. (22) that the changed oscillation pattern in their work might be caused by reactive oxygen species such as singlet O_2 formed by PSII during the illumination with strong laser flashes and X-rays at elevated O_2 pressures.

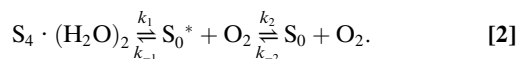
(ii) Misconception in the Interpretation of the UV or the MIMS Data?

The flash-light-induced UV-difference spectra of PSII are composites of events at the donor and the acceptor sides of PSII. The relative spectral contributions of Y_Z and of Mn during the stepwise oxidation of Mn (plus ligand shell) during the transitions from state S_0 via S_1 and S_2 to S_3 have been characterized by several authors, and so was the spontaneous reduction of Y_Z^{ox} and Mn, after S_3 being oxidized to yield S_4 , and the decay in about 1 ms into state S_0 (see ref. 18 and references therein). It has also been established that the wavelength of 360 nm is particularly well suited to monitor Mn transitions because the extent of the reduced-oxidized difference of Y_Z is very small at this wavelength (18, 31). The parallel time course of O_2 -release and UV-absorption transients (360 nm) with a half-time of about 1 ms in WT-PSII also holds in a mutant (D1-D61N) where the half-time is tenfold longer (13 ms) (32). There has been no obvious reason from the literature to doubt (i) the attribution of the UV-millisecond phase to the reduction of Mn and (ii) its parallel time course with O_2 release.

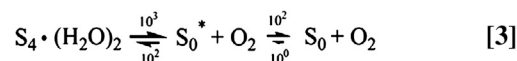
In contrast to all the other techniques, MIMS detects the production of $^{18}\text{O}_2$ from H_2^{18}O directly, the only caveat being that the MIMS signal in response to an O_2 pulse rises rather slowly (instrument-limited half-rise ≈ 10 s), so that a possible slowing of O_2 release may be unnoticed.

(iii) Revision of the Present Understanding?

In line with the above caveat we attempted to reconcile the MIMS results with the previous UV results (23, 30) by assuming that not the Mn reduction and O_2 production, but the effective O_2 release time was slowed down by elevated O_2 pressure and that the driving force for O_2 release comes partially from a conformational change between an initially formed S_0^* state to the more stable S_0 state, a scenario that has been previously proposed by Vos et al. (33). Take the following simplified reaction scheme of the terminal cascade, wherein redox intermediates of the OEC (between states S_4 and S_0), the protonation state of bound water, proton release, and rebinding of substrate water (see reaction 1) are neglected for simplicity.

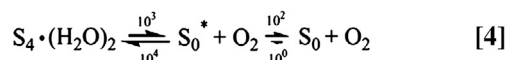


Herein S_0^* denotes a conformationally strained but fully reduced state of the OEC with oxygen already released into the medium, and S_0 its fully relaxed equivalent. All reactions but the one back from S_0^* to S_4 are of first order. Because of the abundance of O_2 , the latter can be considered as pseudofirst order, such that k_{-1} —its magnitude being proportional to the O_2 concentration—comes in s^{-1} , like the other three rate constants. Let us consider the following arbitrary choice of parameters k_i/s^{-1} for the situation at ambient O_2 concentration (0.2 bar):



Then the appearance of O_2 in solution is kinetically limited by the first reaction. Broadly speaking, its exponential rise time is 1 ms and to a lesser extent 10 ms. S_0^* is stabilized by 60 meV compared to S_4 , and S_0 is relative to S_0^* by 120 meV (34). The total stabilization of fully relaxed S_0 is larger, namely 180 meV. Let us now increase the O_2 pressure 100-fold from 0.2 to 20 bars.

Only one parameter depends on the O_2 concentration, namely k_{-1} . Its value increases from 10^2 to 10^4 :



The increase changes the situation dramatically, the rate of net O_2 production is now governed by the second reaction, and it is furthermore delayed by the adverse equilibrium of the first reaction. The rise time of the pulse of O_2 is now about 100 ms instead of 1 ms. In other words, the “millisecond phase” of S_4 reduction is seemingly suppressed (truly slowed down). If the reaction takes place in $H_2^{18}O$ and with $^{16}O_2$ in the gas and liquid phase, then first $^{18}O_2$ appears with the rate k_1 (i.e., in 1 ms) in the solution concomitant with $^{16}O_2$ uptake. The appearance of $^{18}O_2$ is detected by MIMS, whereas the transient intake of $^{16}O_2$ (if present) is not detectable because of the high background signal at $m/z = 32$ under 20 bars of $^{16}O_2$. At 100-fold increased O_2 pressure S_0^* is destabilized by 60 meV relative to S_4 . Because S_0 is still by 120 meV more stable than S_0^* —this is independent of the O_2 pressure—the total driving force for proceeding from S_4 to S_0 is still 60 meV. This is sufficient to expel O_2 into the solution. Rather than to be provided by the very O_2 -liberating step ($S_4 \rightarrow S_0^*$), the forward drive is then provided by the conformational relaxation in the OEC (the transition from S_0^* to S_0). The published UV transients (23) (see also Fig. S8) have revealed that the hypothetical $S_4 \rightarrow S_0^* \rightarrow S_0$ transition would have to last 100 ms or longer.

The above kinetic model predicts that elevated O_2 pressure can suppress the ms phase of Mn reduction (as detected by UV), whereas the appearance of O_2 in solution, detected by MIMS, is seemingly unimpaired. This concept for reconciling the conflicting data on kinetic grounds was tested by the experiments documented in Fig. 4A where a series of 20 light flashes was fired to a dark-adapted sample. The spacing of flashes, 20 ms, was chosen tight enough as to reveal a possible kinetic limitation of the $S_4 \rightarrow S_0^* \rightarrow S_0$ transition. The extent of $^{18}O_2$ release was almost independent of exposing the PSII suspension to either 20 bars O_2 or 17 bars N_2 . This result rules out the above discussed kinetic limitation, in agreement with the TR-XAS finding that the $S_3 \rightarrow S_4 \rightarrow S_0$ kinetic is basically unaffected by elevated O_2 pressure (22).

Consequences for the Energetics of Water Oxidation. MIMS experiments revealed unconstrained O_2 production up to at least 10 bars, i.e., 50-fold elevated partial O_2 pressure, without any indication for the transient retention of O_2 in PSII. O_2 polarography with a bare platinum electrode and other techniques have revealed a half-rise time of 1 ms (see *Introduction*), and rapid exchange between freshly produced O_2 and O_2 in the medium is probable. As a consequence, the dilution of O_2 into the suspending medium adds an entropic term to the free energy of the product side. If the driving force of the O_2 -liberating step was -100 meV under ambient conditions (0.21 bars O_2 , pH 6.5), then the 50-times increased O_2 pressure was expected to raise the backward driving force entropically by 100 meV, such that one expects half of the previous O_2 release into the medium. If the driving force was greater than before, say 160 meV, still 90% of the extent found in air is to be expected. The MIMS data at pH 6.5 and with at least 10 bars dissolved O_2 therefore imply that the terminal step of water oxidation has a driving force greater than 160 meV. Under the likely assumption that the $S_4 \rightarrow S_0$ transition is coupled to the release of at least one proton (see description of reaction 1), the MIMS data under 20 bars O_2 in the gas phase and at pH 5.5 (see Fig. 4B) raise the lower limit for the driving force even to 220 meV. How does this estimate compare with the current ones for the free energies in PSII? The midpoint potential of pheophytin *a* (Pheo *a*) in

Thermosynechococcus elongatus has been recently determined to be $E_m^{pH6.5}(\text{Pheo}/\text{Pheo}^-) = -505$ mV (35), i.e., 100 mV higher than previous estimates (summarized in ref. 36). Based thereupon the midpoint potentials of P680 and Y_Z became also more positive, $E_m(\text{P680}/\text{P680}^{*+}) = +1.210$ V and $E_m(Y_Z/Y_Z^*) = +1.1$ V (35–37). Given that the mean midpoint potential for the oxidation of water under ambient conditions is $+0.8$ V, it appears that there is indeed leeway for such a high driving force for the terminal reaction cascade.

Conclusion

By MIMS we monitored oxygen ($^{18}O_2$) production from water ($H_2^{18}O$) under variation of the oxygen ($^{16}O_2$) pressure around PSII. There was no indication for any inhibition by up to 50-fold increased back pressure of $^{16}O_2$. This result qualifies the previous conclusion to the contrary that has been based on UV-absorption transients (23, 30) and delayed fluorescence (21), and it corroborates results by X-ray absorption transients (22) and visible fluorescence (29). Despite the well-established relation between the millisecond phase of UV-absorption transients (at 360 nm) and the reduction of manganese (see *Introduction*), the MIMS versus UV discrepancy calls for a reevaluation of the difference spectrum of UV-absorption transients as a function of flash number, and in response to low and high oxygen pressure.

It is an important result of the present work that the driving force of the terminal reaction cascade of photosynthetic water oxidation is rather strong, namely at least 160 meV, but taking into account a probable proton release during the $S_4 \rightarrow S_0$ transition, it is even >220 meV (at pH 6.5 and atmospheric conditions). It is obvious that the construction of PSII, by itself, does not impose a narrow constraint to the oxygen content of the atmosphere that can be raised, in principle, by orders of magnitude.

Materials and Methods

Samples and Media. O_2 -evolving PSII-cc were isolated from modified WT cells of *Synechocystis* sp. PCC6803 as described earlier (38). Typical rates of O_2 evolution under continuous illumination were 2,000–3,000 $\mu\text{mol}(O_2) \times \text{mg}(\text{Chl})^{-1} \times \text{h}^{-1}$ (38) (see also *SI Text*). Prior to MIMS measurements PSII-cc were thawed in the dark on ice and diluted to the desired chlorophyll concentrations (5 or 50 μM) with standard medium (100 mM sucrose, 25 mM CaCl_2 , 10 mM NaCl, 1 M glycine betaine, and 50 mM MES at pH 6.7 or 5.5) containing $H_2^{16}O/H_2^{18}O$ mixtures as described below. In some experiments PSII-mf were employed that were prepared from spinach as described previously (39). For the measurements, they were suspended in the following buffer: 150 mM sucrose, 35 mM NaCl, and 40 mM MES at pH 6.5. The rates of O_2 evolution for such samples were 400–500 $\mu\text{mol}(O_2) \times \text{mg}(\text{Chl})^{-1} \times \text{h}^{-1}$.

MIMS Setup for Experiments at Elevated O_2/N_2 Pressure. To perform MIMS measurements (40) of O_2 produced under elevated O_2 pressure, a MIMS reaction cell resisting pressures up to 20 bars was developed (Fig. 1) and connected to the vacuum line of our magnetic sector field isotope-ratio MS (ThermoFinnigan^{plus} XP) via a cooling trap (dry ice/ C_2H_5OH or liquid N_2). The nominal sample space of the chamber was 1 mL, but a volume of 600 μL was used to increase the interface between gas phase and liquid. Gas diffusion into the liquid was further increased by rapid stirring of the suspension. The suspension was separated from the high vacuum (3×10^{-8} mbar) of the MS by a gas-permeable ~ 150 - μm -thick metallic mesh silicon membrane (Framatech GmbH) resting on a porous Teflon support ($\varnothing 3$ mm) (Small Parts Inc.). For monitoring the pressure in a gas phase above the samples, the cover of the reaction chamber was connected to a pressure detector (Huba Control). The MIMS cell was thermostated to 20 °C.

The response of our MIMS setup is linear from ambient pressure up to about 8 bars O_2 (about 99.5% $^{18}O_2$), but then deviates slightly resulting in a dissolved O_2 signal of about 60–80% of what would be expected based on lower pressures (Fig. S1). Possible reasons for this deviation, for example, are (i) pressure effects on the membrane permeability and (ii) a decrease in sensitivity of the mass spectrometer caused by a reduced internal vacuum at high applied pressures. Calibration of the O_2 signals at ambient pressure results in a value of 100 mV ≈ 30 nM $^{18}O_2$ ($m/z = 36$ peak) (for details, see *SI Text*).

Protocol for the detection of O₂ evolution Under Elevated Pressure. H₂¹⁸O (97%; Larodan Fine Chemicals AB) was used to enrich the aqueous sample suspensions with 30–50% of H₂¹⁸O. For this, ¹⁸O-labeled H₂O was added to the reaction mixture that contained either dark-adapted PSII-cc and 2,5-DCBQ as electron acceptor (250- μ M final concentration; added from 20 mM stock solution in ethanol) or PSII-mf and ferricyanide (1 mM). The MIMS chamber was then flushed with the desired gas, sealed, and exposed to elevated O₂/N₂ pressure. The following rise of the dissolved ¹⁶O₂ or ¹⁴N₂ concentrations in the PSII suspension was monitored at $m/z = 32$ and $m/z = 28$, respectively (Fig. 2 and Fig. S2). During this equilibration period (typically about 35–50 min), the reaction mixture was stirred in darkness.

PSII-cc were excited via the sapphire window of the MIMS cell (Fig. 1) with a group of short saturating Xe flashes provided by one of the following Xe flash lamps: Perkin Elmer, LS-1130-4 (max. 50 Hz; \sim 5- μ s half-width) or EG&G, model PS 302, light pack FY-604 (max. 10 Hz; \sim 15- μ s half-width). The experiments on spinach PSII-mf (Fig. 5 A and B) were performed employing a frequency doubled Nd-YAG laser (Continuum Inlite II-20; 532 nm).

- Kok B, Forbush B, McGloin M (1970) Cooperation of charges in photosynthetic O₂ evolution. *Photochem Photobiol* 11:457–476.
- Joliot P, Barbieri G, Chabaud R (1969) Un nouveau modele des centres photochimiques du systeme II. *Photochem Photobiol* 10:309–329.
- Messinger J, Renger G (2008) *Primary Processes of Photosynthesis, Part 2 Principles and Apparatus*, ed G Renger (RSC Publishing, Cambridge, UK), pp 291–351.
- Siegbahn PEM (2009) Structures and energetics for O₂ formation in photosystem II. *Acc Chem Res* 42:1871–1880.
- Dau H, Haumann M (2008) The manganese complex of photosystem II in its reaction cycle—Basic framework and possible realization at the atomic level. *Coord Chem Rev* 252:273–295.
- Junge W, Haumann M, Ahlbrink R, Mulikdjanian A, Clausen J (2002) Electrostatics and proton transfer in photosynthetic water oxidation. *Philos T R Soc Lon B* 357:1407–1417.
- Rappaport F, Blanchard-Desce M, Lavergne J (1994) Kinetics of electron transfer and electrochromic change during the redox transitions of the photosynthetic oxygen evolving complex. *Biochim Biophys Acta* 1184:178–192.
- Haumann M, et al. (2005) Photosynthetic O₂ formation tracked by time-resolved X-ray experiments. *Science* 310:1019–1021.
- Etienne AL (1968) Etude de l'etape thermique de l'emission photosynthetique d'oxygene par une methode d'ecoulement. *Biochim Biophys Acta* 153:895–897.
- Razeghifard MR, Pace RJ (1999) EPR kinetic studies of oxygen release in thylakoids in PSII membranes: a kinetic intermediate in the S₃ to S₀ transition. *Biochemistry* 38:1252–1257.
- Strzalka K, Walczak T, Sarna T, Swartz HM (1990) Measurement of time-resolved oxygen concentration changes in photosynthetic systems by nitroxide-based EPR oximetry. *Arch Biochem Biophys* 281:312–318.
- Clausen J, Debus RJ, Junge W (2004) Time-resolved oxygen production by PSII: Chasing chemical intermediates. *Biochim Biophys Acta* 1655:184–194.
- Jursinic PA, Dennenberg RJ (1990) Oxygen release time in leaf disks and thylakoids of peas and photosystem II membrane fragments of spinach. *Biochim Biophys Acta* 1020:195–206.
- Meunier PC, Popovic R (1991) The time for oxygen release in photosynthesis: reconciliation of flash polarography with other measurement techniques. *Photosynth Res* 28:33–39.
- Lavergne J (1989) Mitochondrial responses to intracellular pulses of photosynthetic oxygen. *Proc Natl Acad Sci USA* 86:8768–8772.
- Babcock GT, Blankenship RE, Sauer K (1976) Reaction kinetics for positive charge accumulation on the water side of chloroplast photosystem II. *FEBS Lett* 61:286–289.
- Razeghifard MR, Klughammer C, Pace RJ (1997) Electron paramagnetic resonance kinetic studies of the S states in spinach thylakoids. *Biochemistry* 36:86–92.
- Lavergne J (1991) Improved UV-visible spectra of S-state transitions in the photosynthetic oxygen evolving system. *Biochim Biophys Acta* 1060:175–188.
- Renger G, Hanssum B (1992) Studies on the reaction coordinates of the water oxidase in PSII membrane-fragments from spinach. *FEBS Lett* 299:28–32.
- Karge M, Irrgang K-D, Renger G (1997) Analysis of the reaction coordinate of photosynthetic water oxidation by kinetic measurements of 355 nm absorption changes at different temperatures in photosystem II preparations suspended in either H₂O or D₂O. *Biochemistry* 36:8904–8913.
- Clausen J, Junge W, Dau H, Haumann M (2005) Photosynthetic water oxidation at high O₂ backpressure monitored by delayed chlorophyll fluorescence. *Biochemistry* 44:12775–12779.
- Haumann M, Grundmeier A, Zaharieva I, Dau H (2008) Photosynthetic water oxidation at elevated dioxygen partial pressure monitored by time-resolved X-ray absorption measurements. *Proc Natl Acad Sci USA* 105:17384–17389.
- Clausen J, Junge W (2004) Detection of an intermediate of photosynthetic water oxidation. *Nature* 430:480–483.
- Dau H, Haumann M (2006) Photosynthetic oxygen production—Response. *Science* 312:1471–1472.
- Junge W, Clausen J (2006) Photosynthetic oxygen production. *Science* 312:1470–1470.
- Penner-Hahn JE, Yocum CF (2006) Photosynthetic oxygen production—Response. *Science* 312:1470–1471.
- Penner-Hahn JE, Yocum CF (2005) Biochemistry—The photosynthesis “oxygen clock” gets a new number. *Science* 310:982–983.
- Raven JA, Larkum AWD (2007) Are there ecological implications for the proposed energetic restrictions on photosynthetic oxygen evolution at high oxygen concentrations? *Photosynth Res* 94:31–42.
- Kolling DRJ, Brown TS, Ananyev G, Dismukes GC (2009) Photosynthetic oxygen evolution is not reversed at high oxygen pressures: Mechanistic consequences for the water-oxidizing complex. *Biochemistry* 48:1381–1389.
- Clausen J, Junge W (2008) The inhibitory effects of acidification and augmented oxygen pressure on water oxidation. *Photosynth Res* 98:229–233.
- Dekker JP, van Gorkom HJ, Wensink J, Ouweland L (1984) Absorbance difference spectra of the successive redox states of the oxygen-evolving apparatus of photosynthesis. *Biochim Biophys Acta* 767:1–9.
- Hundelt M, Hays A-MA, Debus RJ, Junge W (1998) Oxygenic photosystem II: The mutation D1-D61N in *Synechocystis* sp PCC 6803 retards S-state transitions without affecting electron transfer from Y₂ to P680⁺. *Biochemistry* 37:14450–14456.
- Vos MH, van Gorkom HJ, van Leeuwen PJ (1991) An electroluminescence study of stabilization reactions in the oxygen-evolving complex of photosystem II. *Biochim Biophys Acta* 1056:27–39.
- Renger G (1977) A model for the molecular mechanism of photosynthetic oxygen evolution. *FEBS Lett* 81:223–228.
- Kato Y, Sugiura M, Oda A, Watanabe T (2009) Spectroelectrochemical determination of the redox potential of pheophytin a, the primary electron acceptor in photosystem II. *Proc Natl Acad Sci USA* 106:17365–17370.
- Rappaport F, Guergova-Kuras M, Nixon PJ, Diner BA, Lavergne J (2002) Kinetics and pathways of charge recombination in photosystem II. *Biochemistry* 41:8518–8527.
- Rappaport F, Diner BA (2008) Primary photochemistry and energetics leading to the oxidation of the (Mn)₄Ca cluster and to the evolution of molecular oxygen in Photosystem II. *Coord Chem Rev* 252:259–272.
- Clausen J, et al. (2001) Photosynthetic water oxidation in *Synechocystis* sp PCC6803: mutations D1-E189K, R and Q are without influence on electron transfer at the donor side of photosystem II. *Biochim Biophys Acta* 1506:224–235.
- Berthold DA, Babcock GT, Yocum CF (1981) A highly resolved, oxygen-evolving photosystem II preparation from spinach thylakoid membranes. *FEBS Lett* 134:231–234.
- Beckmann K, Messinger J, Badger MR, Wydrzynski T, Hillier W (2009) On-line mass spectrometry: membrane inlet sampling. *Photosynth Res* 102:511–522.